



A Facile Sol–Gel Process for Synthesis of ZnWO₄ Nanoparticles with Enhanced Band Gap and Study of Its Photocatalytic Activity for Degradation of Methylene Blue

Mahbobeh Rahmani¹ · Tahereh Sedaghat¹

Received: 8 August 2018 / Accepted: 24 September 2018 / Published online: 12 October 2018
© Springer Science+Business Media, LLC, part of Springer Nature 2018

Abstract

ZnWO₄ nanoparticles were synthesized by a facile sol–gel method using Zn(CH₃COO)₂ and Na₂WO₄. The as-prepared ZnWO₄ was characterized by several techniques: XRD, FTIR, TEM, FESEM, EDS, BET, PL and DRS. The effects of pH and calcined temperatures were investigated on the crystal structure of the ZnWO₄ photocatalyst. Results showed that pure ZnWO₄ was synthesized in pH 6 and calcined temperature 500 °C for 5 h. The synthesized ZnWO₄ nanoparticles have a mean diameter less than 100 nm and the band gap energy are about 3.20 eV. ZnWO₄ nanoparticles showed efficient photocatalytic activity for the degradation of methylene blue under ultraviolet light irradiation. The apparent rate constant (k) of photodegradation reaction was obtained as $1.62 \times 10^{-2} \text{ min}^{-1}$.

Keywords Zinc tungstate · Photocatalytic activity · Methylene blue · Sol–gel

1 Introduction

One of the main contaminants of water is organic dyes used in industries such as textiles, plastic and paper. Organic dyes have high stability against temperature, chemicals and bacterial attack. So far many methods have been investigated for the treatment of these dyes from water [1–3]. Nowadays, the purification of the water and wastewater from dyes by photocatalysts has attracted much attention [4–6]. Photodegradation process by semiconductors leads to complete mineralization of various organic compounds to CO₂, water, mineral acids [7]. Among different semiconductors, ZnWO₄ is a nontoxic important and attractive inorganic material with excellent properties and many potential application in various fields such as scintillating materials, solid-state laser host, photocatalysts, gas and humidity sensors, optical fibers and so on. ZnWO₄ is an environment–friendly semiconductor with a relatively wide direct bandgap; on the order of 3.8–5.7 eV [8], which has photocatalytic activity for degradation of organic materials under UV irradiation. ZnWO₄ is

a member of metal tungstates that crystallizes in the monoclinic wolframite structure with C2h point group symmetry and P2/c space group. The structure of this compound consists of zig-zag metal–oxygen chains that are composed of edge-sharing ZnO₆ and WO₆ octahedra [8–10].

Until now, ZnWO₄ has been synthesized by various methods such as solid state, sol–gel, molten salt, template, hydrothermal and microwave [11–19]. The improvement of photocatalytic activity of ZnWO₄ is prevented by its large band gap energy and recombination of photoinduced electron–hole pairs. One strategy for the enhancement of the photocatalytic activity of ZnWO₄ is nonmetal or transition metals doping to extend the photoresponse region. Huang et al. synthesized ZnWO₄ doped with chlorine as photocatalysts by hydrothermal process [20]. They succeed to reduce the band gap energy of ZnWO₄ to 3.68 eV. Also Liu et al. synthesized B-doped ZnWO₄ nanorods with $E_g = 3.62 \text{ eV}$ [21]. Arin et al. synthesized La-doped ZnWO₄ by hydrothermal method and reduced the band gap energy of ZnWO₄ to 3.11 eV by 20% La-doped ZnWO₄ [22]. Another way to reduce the band gap and improve the activity of ZnWO₄ as a photocatalyst is to control the morphology. In this work, we report a simple and inexpensive sol–gel method for synthesis of ZnWO₄ photocatalyst with suitable band gap energy without use of any dopant. The pH and temperature-dependant

✉ Tahereh Sedaghat
tsedaghat@scu.ac.ir

¹ Department of Chemistry, College of Sciences, Shahid Chamran University of Ahvaz, Ahvaz, Iran

structure and photocatalytic activity of the resultant photocatalyst are investigated.

2 Experimental

2.1 Materials

All the reagents used in this research were of analytical grade without further purification. All aqueous solutions were prepared by using deionized water. $\text{Zn}(\text{CH}_3\text{COO})_2 \cdot 2\text{H}_2\text{O}$ (Assay 99.5%), $\text{Na}_2\text{WO}_4 \cdot 2\text{H}_2\text{O}$ (assay 99%), ammonia (25 wt% NH_3), hydrochloric acid (37 wt% HCl), EtOH (assay 99.7–100%), methylene blue, and urea were purchased from the Merck company.

2.2 Characterization Methods

The crystal structures of the samples and chemical composition were characterized using X-ray diffractometer (XRD; Philips PW1730) with monochromatic $\text{Cu K}\alpha$ radiation ($\lambda = 0.15406 \text{ nm}$) in the 2θ range from 10° to 80° . The UV–Vis diffuse–reflectance spectrum (DRS) was recorded using a Shimadzu (MPC-2200) spectrophotometer in range of 200–1100 nm to evaluate the band gap energy of sample. The Field Emission-Scanning Electron microscopy (FESEM) was performed using a MIRA3 TESCAN Microscope at an accelerating voltage of 15 kV together with an energy dispersive X-ray (EDX) to analysis the elements composition of samples. For studying the morphology of the prepared samples, Transmission Electron Microscopy (TEM) images were carried out using an FM10C-100 kV Series Microscope (zeiss company Germany).

The Brunauer–Emmett–Teller (BET) surface area of the product was measured by micromeritics (Gemini). The absorbed gas was nitrogen. Fourier transform infrared spectra (FT-IR) were recorded by a FT BOMEM MB102 spectrophotometer in the range of $400\text{--}4000 \text{ cm}^{-1}$ using the KBr discs. Absorption of solutions in photocatalytic experiments were monitored using T70 UV–Vis spectrophotometer (PG Instruments Ltd).

2.3 Preparation of Nanosized ZnWO_4 Photocatalyst

Nanosized ZnWO_4 photocatalyst was prepared by using sol–gel method. A solution of $\text{Zn}(\text{CH}_3\text{COO})_2 \cdot 2\text{H}_2\text{O}$ (0.025 mol) in 30 mL EtOH was prepared and then 1 mL concentrated HCl in EtOH (30 mL) was added. This solution was ultrasonicated for 30 min. After that, the pH of the solution was adjusted to 3, 6 or 8 by ammonia and diluted HCl solutions. Then, the required amount of $\text{Na}_2\text{WO}_4 \cdot 2\text{H}_2\text{O}$ (with molar ratio W to Zn 1.0%) was dissolved in 30 mL of deionized water. This solution was dropwisely added into the

first one under vigorous stirring. Then the resulting white colloidal suspension was stirred for 1 h continuously and it was aged for 48 h in the room temperature until formation of xerogel. The gel was filtered, washed with 80 mL deionized water and ethanol (1:1) and dried in oven at 80°C for 2 h. Then, the dried gel was calcined at different temperatures (400°C , 500°C or 600°C) for 5 h under heating rate of $10^\circ\text{C min}^{-1}$. Finally, the calcined product was ground in an agate mortar to obtain a fine powder.

2.4 Photocatalytic Experiments

The photocatalytic activities of ZnWO_4 nanocrystals were evaluated through photodegradation of methylene blue (MB) under 15 W mercury lamp irradiation (Philips, 010 UVA, TL-D). Different amounts of the photocatalyst (0.1, 0.15, 0.2 and 0.3 g) were dispersed in an aqueous solution of MB (16 mg L^{-1} , 100 mL) at room temperature. Before

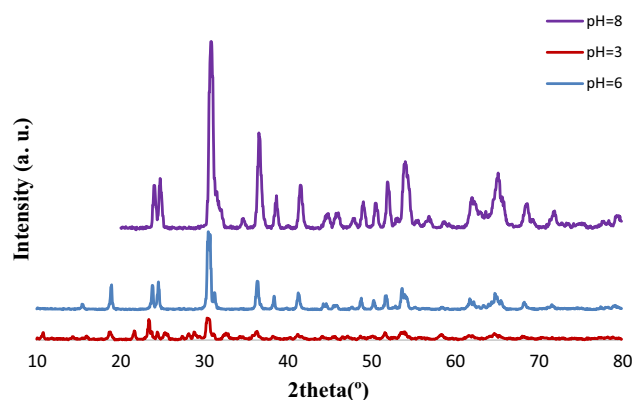


Fig. 1 XRD patterns of the samples obtained by sol–gel procedure with different pH values

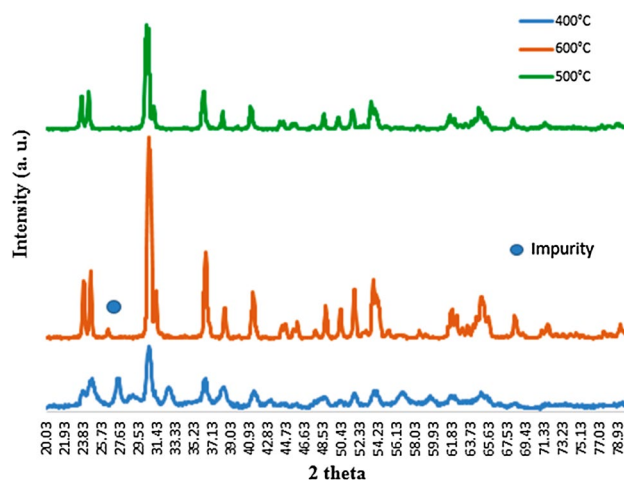


Fig. 2 XRD patterns of the samples obtained by sol–gel procedure with different calcinated temperatures (400°C , 500°C and 600°C)

illumination, the suspension was continuously stirred in the dark for one hour to establish adsorption–desorption equilibrium. The change in the concentration of the residual dye was detected using UV–Vis spectrophotometer. The absorbance value of methylene blue was determined at 664 nm. The concentration of the dye after adsorption was taken as the initial concentration of the pollutant. Then the solution was irradiated under magnetic stirring by the lamp was positioned 10 cm above from the surface of the suspension. At different irradiation time intervals, 3 mL of the solution was collected and it was centrifuged at 5000 rpm for 20 min. The concentration of remaining dye in collected solution

was measured by monitoring the absorbance of the extracted solution in the quartz cell each 30 min.

3 Results and Discussion

3.1 Characterization

ZnWO₄ were synthesized by sol–gel process and the phase purity of products is examined by XRD. Figure 1 shows the XRD patterns of the samples prepared at different pH values. When the pH value is 3, the Na₂W₄O₁₃ (JCPDS card

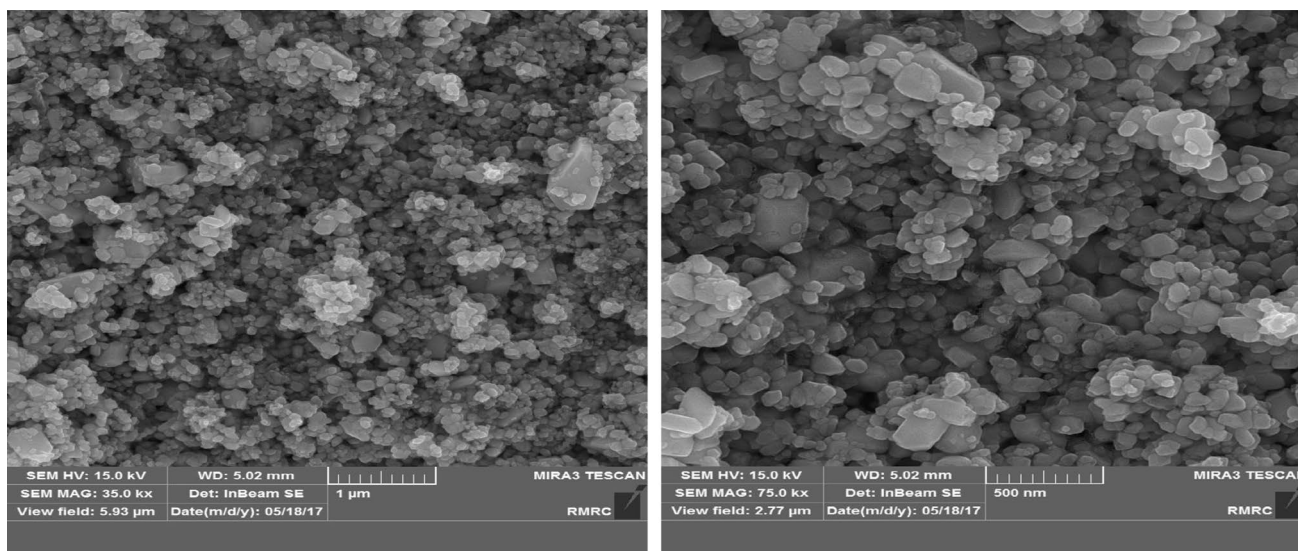


Fig. 3 FESEM images of the ZnWO₄ nanoparticles

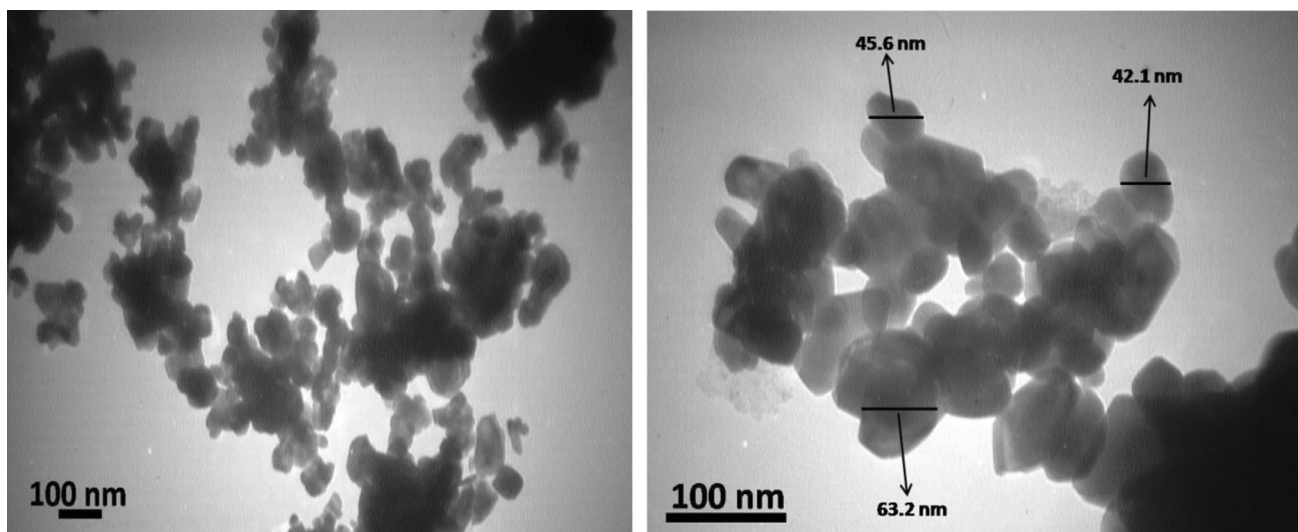


Fig. 4 TEM Images of the ZnWO₄ nanoparticles

NO. 98-000-2045) and $\text{Na}_2\text{W}_2\text{O}_7$ (JCPDS card No. 98-000-0983) phases are formed with ZnWO_4 phase. The polytungstates can be regarded as oxide clusters and synthesized by the solid-state reaction technique in high temperatures [23–25]. The $\text{Na}_2\text{W}_4\text{O}_{13}$ consists of the tungsten oxide layers and sodium ions between the layers [23]. According to the XRD pattern of the sample obtained at pH value of 6, all diffraction peaks are indexed to the pure monoclinic ZnWO_4 (JCPDS card NO. 15-0774) and the diffraction peaks of the side products are disappeared. The sharp peaks indicate that the products are well crystalline. From the other

point, at pH value of 8, the ZnO phase (JCPDS card NO. 98-001-1316) is formed with ZnWO_4 phase. These results show that pure ZnWO_4 phase can be provided via controlling pH value and the suitable pH for the synthesis of the pure ZnWO_4 is 6.

Also, the effect of the calcination temperature on the crystal structure of the products was investigated. Figure 2 demonstrates the XRD spectra of the samples calcinated in different temperatures (400 °C, 500 °C and 600 °C). As a comparison, pure ZnWO_4 was obtained in 500 °C. It was found that other peak impurities were detected in the XRD

Fig. 5 EDX spectrum of the ZnWO_4 nanoparticles

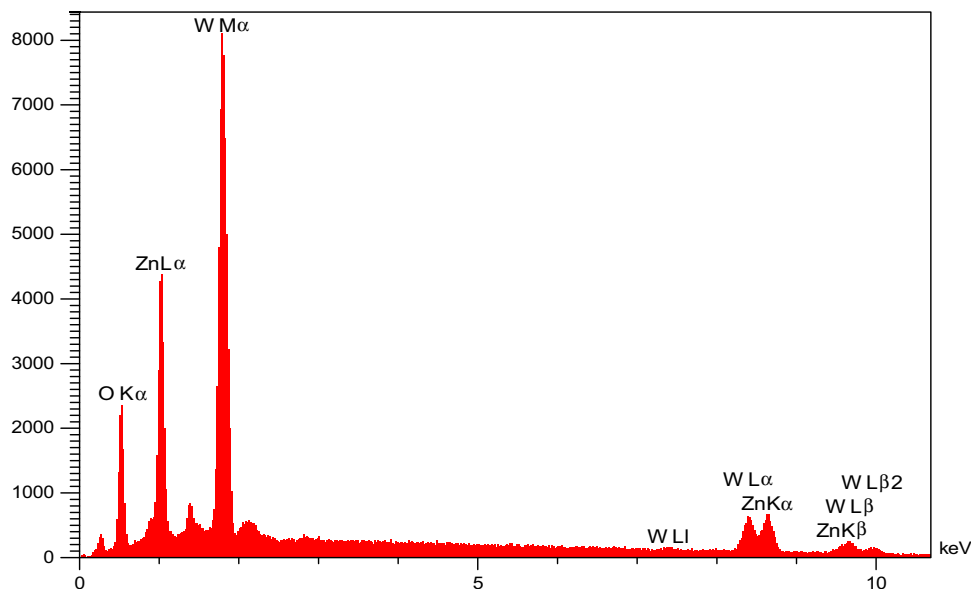
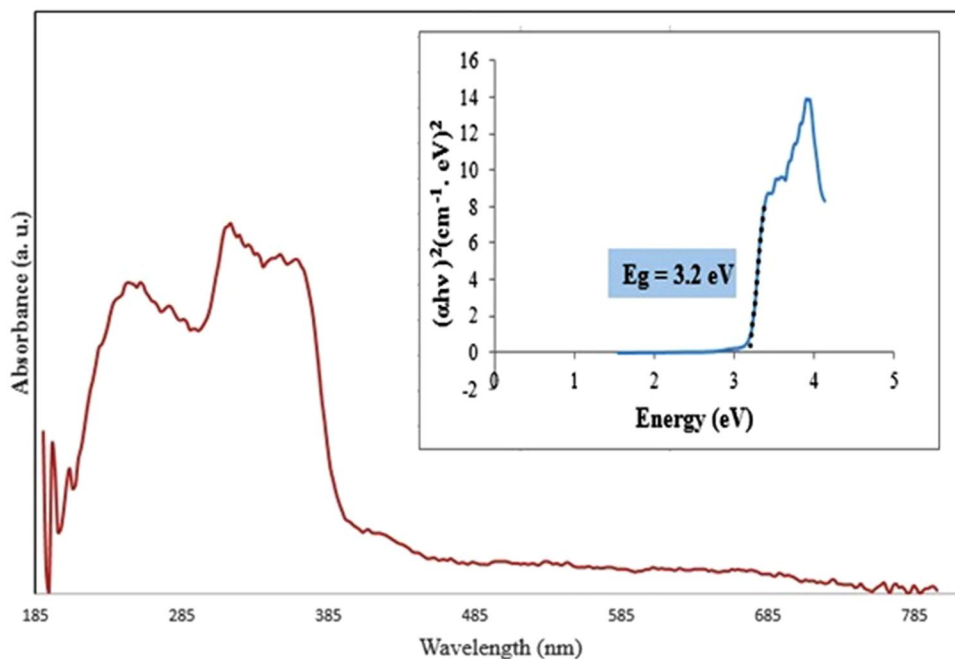


Fig. 6 UV–Vis diffuse reflectance absorption spectrum (DRS) of the ZnWO_4 photocatalyst calcined at 500 °C for 4 h. Insert shows the plot of $(\alpha h\nu)^2$ vs. the photon energy (eV)



patterns of the samples that were calcinated in 400 °C and 600 °C.

Figure 3 shows FESEM images of the pure ZnWO_4 sample prepared at pH 6. The particle size of as-prepared ZnWO_4 is below 100 nm. In order to determine the morphology and exact size of the ZnWO_4 nanoparticles, TEM analysis was used. Figure 4 shows the TEM images of the ZnWO_4 nanoparticles. According to these images, the nanoparticles have an average diameter about 26–78 nm which are in agreement with FESEM results. On the basis of BET results, the surface area of ZnWO_4 nanoparticles was $5.8161 \text{ m}^2 \text{ g}^{-1}$.

The EDX spectroscopic data exhibits that the final product is pure phase ZnWO_4 without any other elements. The material is composed of Zn, W and O with an atom ratio of close to 1:1:4. EDX spectrum of the ZnWO_4 nanoparticles is shown in Fig. 5.

Figure 6 displays UV–Vis DRS spectra of pure ZnWO_4 . Electronic spectral properties are affected by the crystal sizes and morphologies of the final ZnWO_4 powders. As the Fig. 6 shows, the strong absorbance was observed only in the UV region for synthesized ZnWO_4 . The band gap energy (E_g) of the ZnWO_4 can be estimated from a plot of $(\alpha h\nu)^2$ vs. photon energies (eV) using the following equations [23, 26]:

Fig. 7 The room temperature photoluminescence (PL) emission spectrum of ZnWO_4

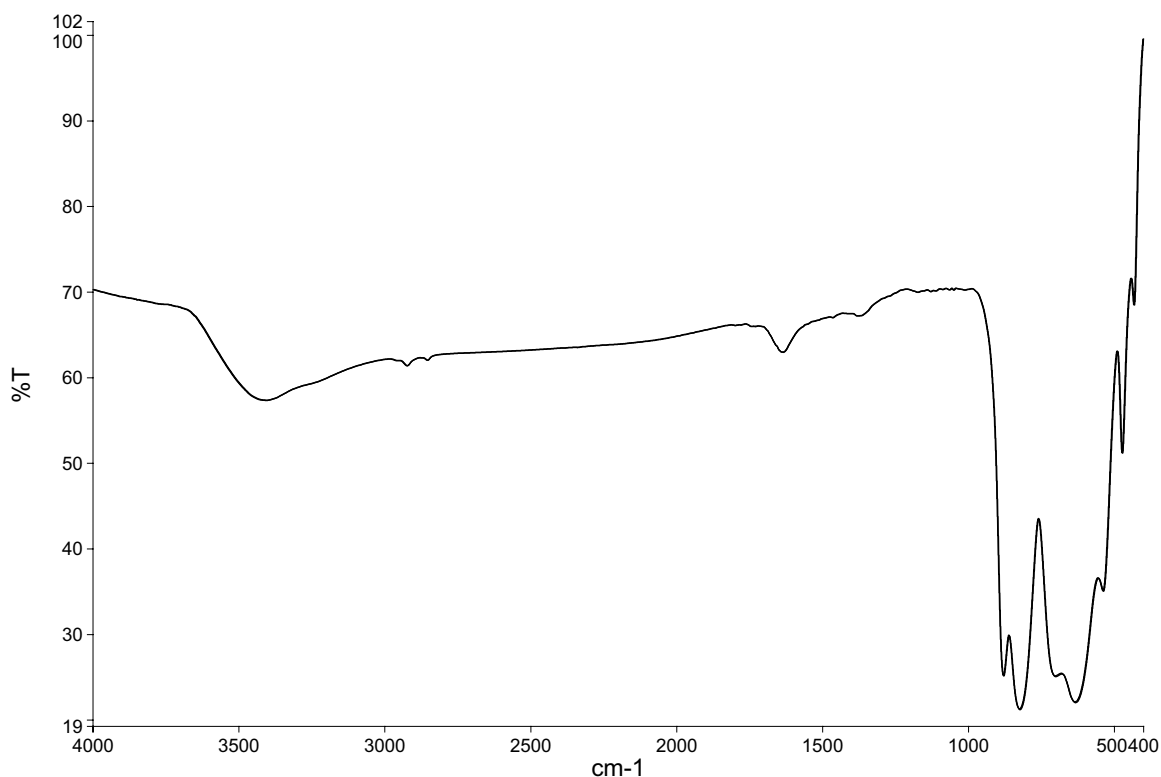
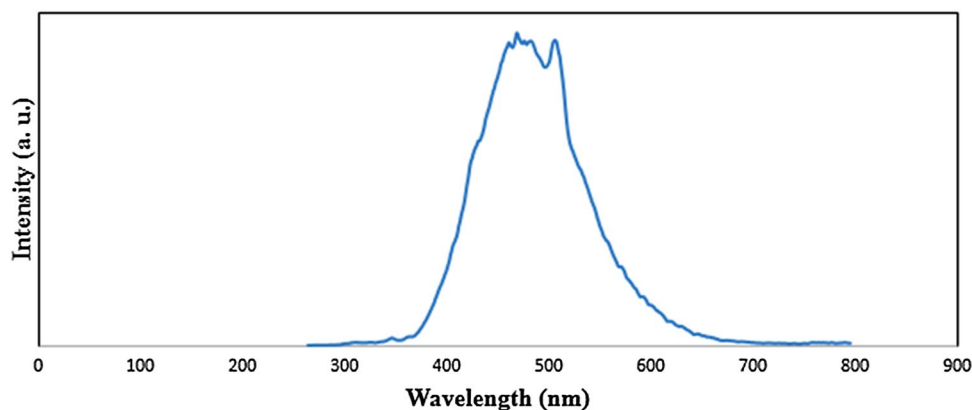


Fig. 8 IR spectrum of synthesized ZnWO_4

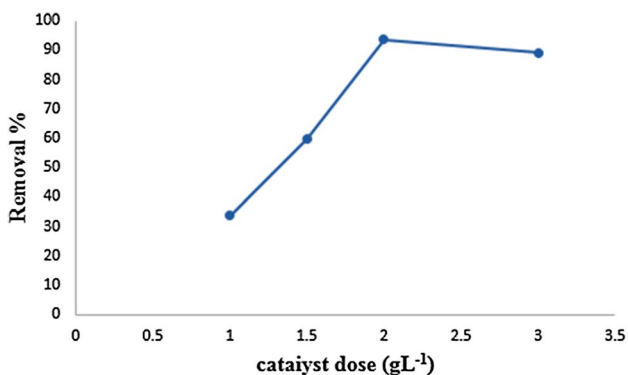


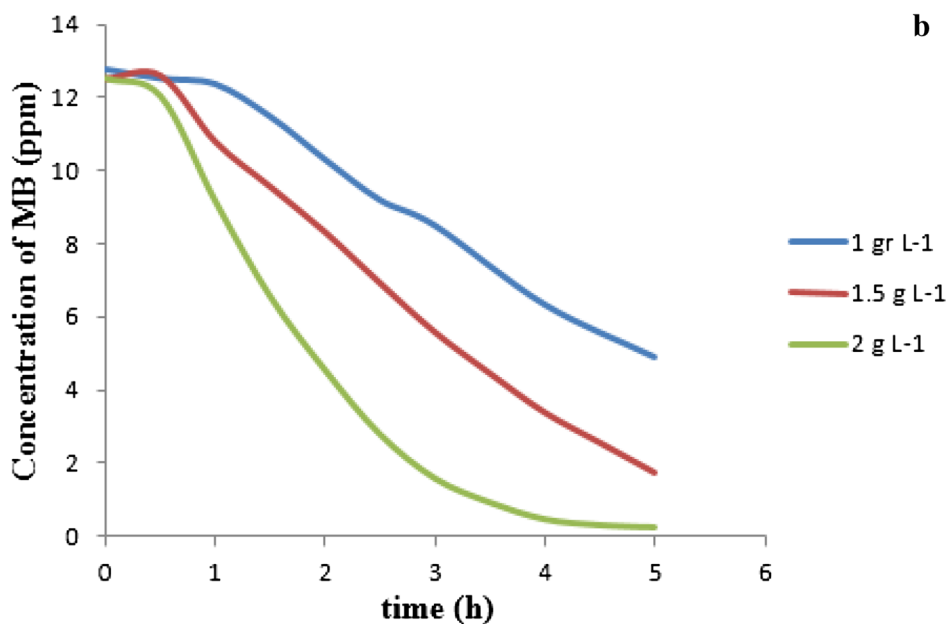
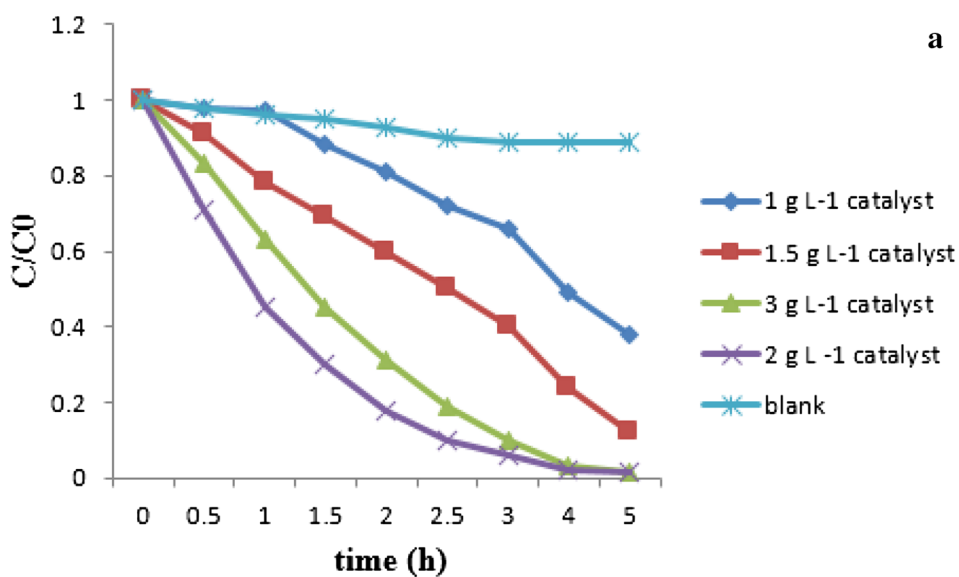
Fig. 9 Effect of catalyst dose on the degradation of MB aqueous solution under UV irradiation

$$(\alpha h\nu) = A(h\nu - E_g)^n \quad n = 1/2, 2, 3/2, 3 \quad (1)$$

$$E = \frac{hc}{\lambda} = \frac{1240}{\lambda} \quad (2)$$

where α , A , ν , c , h , λ and E_g are the absorption coefficient, proportionality constant, light frequency, the velocity of light ($3 \times 10^8 \text{ ms}^{-1}$), the planck's constant ($4.14 \times 10^{-15} \text{ eV}$), the wavelength (nm) and the band gap energy (eV), respectively. That $n = 1/2, 2, 3/2, 3$ are for a direct allowed transition, for an indirect allowed transition, for a direct forbidden transition and for an indirect forbidden transition, respectively. The band gap energy (E_g) of the ZnWO_4 can

Fig. 10 a Photocatalytic degradation of MB in presence of the different amounts of ZnWO_4 , b residual concentration of MB using different amounts of ZnWO_4 under UV irradiation



be determined by extrapolation of linear part of the curve to the $h\nu$ axis intercept that it was specified to be 3.20 eV.

Figure 7 shows the room temperature photoluminescence (PL) emission spectrum of ZnWO_4 . It can be observed that the pure ZnWO_4 nanoparticles exhibit a broad peak in the range of 300–700 nm, centered around 468 nm when excited in 254 nm. This intrinsic luminescence might be due to charge transition between the O_{2p} orbitals and the empty d orbitals of the central W^{6+} ions in the WO_6 group [9, 14, 27–29].

The FTIR spectrum of the ZnWO_4 was shown in Fig. 8. The stretching vibrations of W–O occur at 823 cm^{-1} and 879 cm^{-1} [20, 30, 31]. The bands at 471 cm^{-1} and 431 cm^{-1} can be due to the bending and stretching vibrations of Zn–O. The broad band about 3404 cm^{-1} and the band at 1634 cm^{-1} are attributed to the stretching and bending vibrations of O–H [20].

3.2 Photocatalytic Performance

The photocatalytic activity of the as-prepared ZnWO_4 nanoparticles were evaluated by the photodegradation of methylene blue aqueous solution. The effect of the catalyst dose on the photodegradation was investigated by different amounts of photocatalyst. The MB removal percents 33.57, 59.70, 93.51 and 89.18 were obtained for the catalyst doses 1 g L^{-1} , 1.5 g L^{-1} , 2 g L^{-1} and 3 g L^{-1} , respectively, after 3 h irradiation. It was revealed that 2 g L^{-1} of ZnWO_4 has the highest removal percent of the dye from solution. Figure 9 shows the effect of catalyst dose on the degradation of MB aqueous solution under UV irradiation.

Figure 10a, b shows the photocatalytic degradation of MB solution as a function of irradiation time over different amounts of photocatalyst. The blank test indicates that the photolysis of MB can be ignored. The results show the photocatalytic activity enhances with increasing the amount of ZnWO_4 to 2 g L^{-1} .

Figure 11 shows the spectral changes during the photodegradation of MB aqueous solution (16 mg L^{-1}) in the presence of 2 g L^{-1} of ZnWO_4 at various time intervals under UV light irradiation. MB shows an apparent absorbance at wavelength 664 nm that with increasing the irradiation time, an obvious decreasing appears in the intensity of this peak. Furthermore, during the photodegradation process, the absorption peak clearly shows a blue shift. These findings are in accordance with the results reported by Huang et al. [20] and Zhang et al. [32]. They investigated the photoactivity enhancement of ZnWO_4 photocatalysts doped with chlorine and photooxidative N-demethylation of methylene blue (MB) in aqueous TiO_2 dispersions under UV irradiation, respectively. They found that MB degradation occurs via N-demethylation. The color of dye solution changes from deep blue to light blue and then becomes colorless.

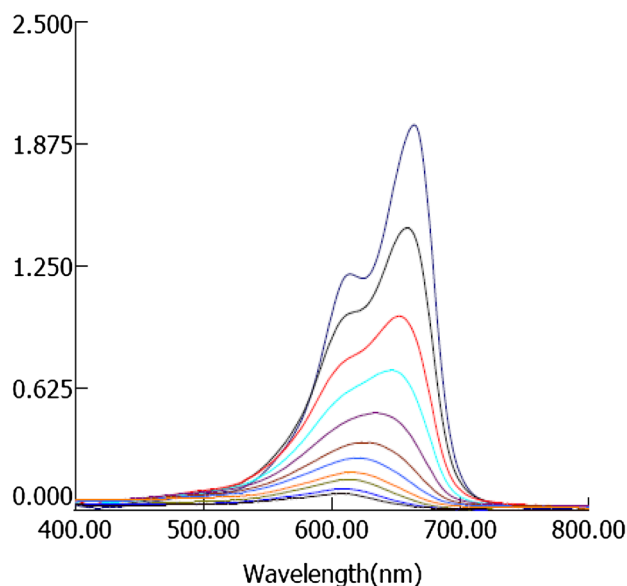


Fig. 11 UV–Vis spectral changes of MB aqueous solution by ZnWO_4

The color of MB solution becomes less intense when all or part of methyl or methylamine groups degrades. Therefore N-demethylation and oxidative degradation occurs during the photodegradation process of MB.

The first order linear relationship was observed by the plot of the $\ln C_0/C$ vs. irradiation time (min) in Fig. 12. C_0 and C are the concentrations of MB at time t_0 and t , respectively. From the graph, the apparent rate constant (k) of the photodegradation reaction is $1.62 \times 10^{-2}\text{ min}^{-1}$ and the linear fit (R^2) is 0.998.

The reusability tests for MB photodegradation using ZnWO_4 were carried out to investigate the photocatalytic stability of as-prepared catalyst. After every 60 min of photodegradation, the ZnWO_4 was separated and washed with deionized water and dried. Figure 13 shows that the

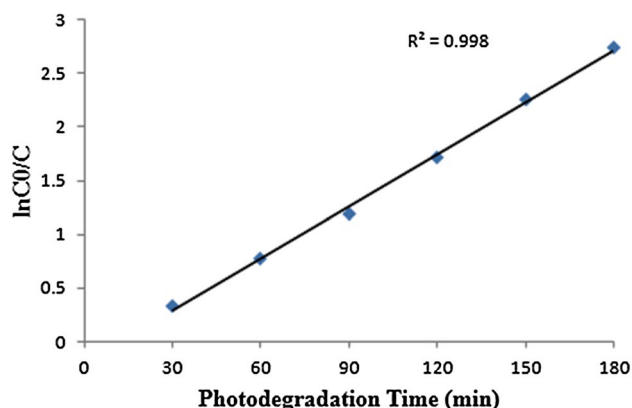


Fig. 12 Photocatalytic kinetic graph for the degradation of MB by ZnWO_4 under UV irradiation

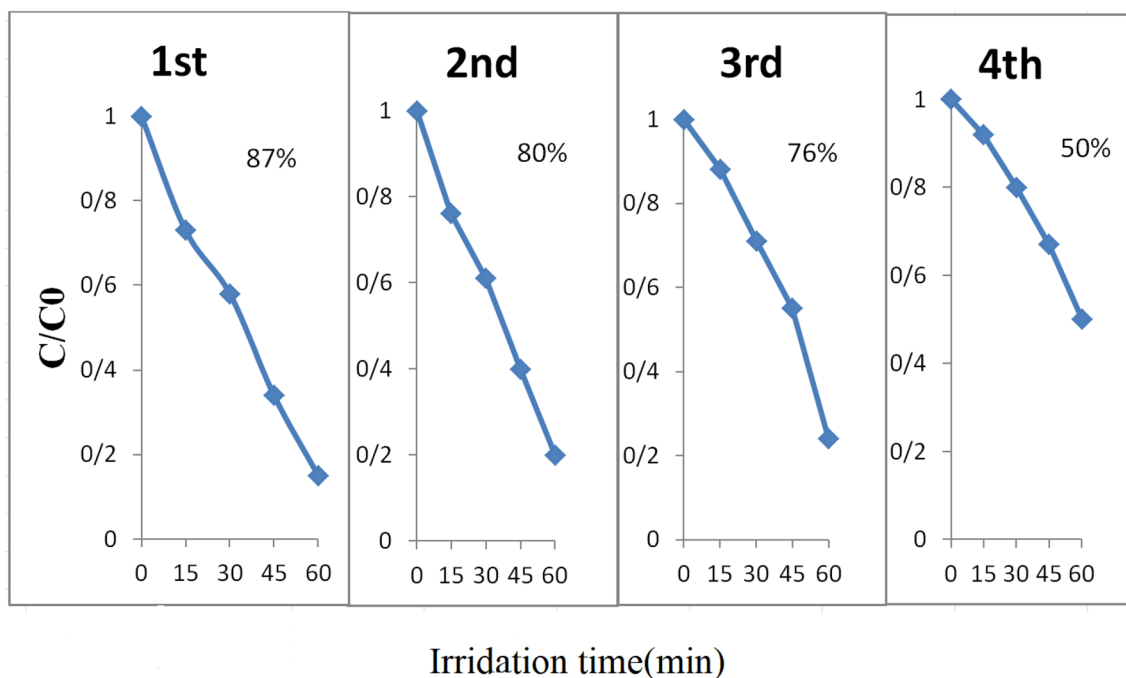


Fig. 13 Cycling runs in the photocatalytic degradation of MB in presence of ZnWO_4

photodegradation efficiency of ZnWO_4 was still more than 75% after three cycles and the catalyst did not exhibit any significant loss of activity, but after fourth cycle, it was 50%. The slight decrease in activity after three cycles, confirming that as-prepared catalyst is stable during the photocatalytic oxidation of the MB molecules.

4 Conclusion

ZnWO_4 photocatalyst prepared via a simple sol–gel process exhibited high photocatalytic activity for the degradation of the MB aqueous solution under UV irradiation. The pH value and the calcined temperature were affective on the structure of the ZnWO_4 nanoparticles. The pure nano-sized ZnWO_4 with average diameter about 26–78 nm was synthesized at pH value 6 and calcined temperature 500 °C. The band gap energy of as-prepared ZnWO_4 was 3.20 eV without the use of any dopant and these nanoparticles degrade MB with $k = 1.62 \times 10^{-2} \text{ min}^{-1}$. As a comparison, Huang et al. obtained the band gap 3.70 eV and 3.68 eV, respectively for pure ZnWO_4 and chlorine doped ZnWO_4 synthesized by hydrothermal method with particle sizes 30–50 nm [20]. They also obtained the reaction rate constants, k , for MB degradation by these materials 0.38×10^{-2} and 1.54×10^{-2} , respectively. Therefore, ZnWO_4 nanoparticles synthesized herein by a facile method show an enhanced band gap and improved catalytic activity. These results are promising for the enhancement of photocatalytic properties of this

photocatalyst alongside organic/inorganic metal doping to extend the light absorption spectrum from UV to visible light.

Acknowledgements Support of this work by Shahid Chamran University of Ahvaz, Iran (Grant No. 1396) is gratefully acknowledged.

References

1. E. Forgacs, T. Cserhati, G. Oros, *Environ. Int.* **30**, 953 (2004)
2. H.S. Rai, M.S. Bhattacharyya, J. Singh, T. Bansal, P. Vats, U. Banerjee, *Crit. Rev. Environ. Sci. Technol.* **35**, 219 (2005)
3. V. Gupta, *J. Environ. Manage.* **90**, 2313 (2009)
4. P. Sathishkumar, R. Sweena, J.J. Wu, S. Anandan, *Chem. Eng. J.* **171**, 136 (2011)
5. P.W. Koh, M.H.M. Hatta, S.T. Ong, L. Yuliati, S.L. Lee, *J. Photochem. Photobiol. A* **332**, 215 (2017)
6. D. Maučec, A. Šuligoj, A. Ristić, G. Dražić, A. Pintar, N.N. Tušar, *Catal. Today* **310**, 32 (2018)
7. A.L. Linsebigler, G. Lu, J.T. Yates Jr., *Chem. Rev.* **95**, 735 (1995)
8. E.D. Bøjesen, K.M. Jensen, C. Tyrsted, A. Mamakhel, H.L. Andersen, H. Reardon, J. Chevalier, A.-C. Dippel, B.B. Iversen, *Chem. Sci.* **7**, 6394 (2016)
9. C. Zhang, H. Zhang, K. Zhang, X. Li, Q. Leng, C. Hu, *ACS Appl. Mater. Interfaces* **6**, 14423 (2014)
10. G. Huang, C. Zhang, Y. Zhu, *J. Alloys Compd.* **432**, 269 (2007)
11. A. Phani, M. Passacantando, L. Lozzi, S. Santucci, *J. Mater. Sci.* **35**, 4879 (2000)
12. X. Jiang, J. Ma, J. Liu, Y. Ren, B. Lin, J. Tao, X. Zhu, *Mater. Lett.* **61**, 4595 (2007)
13. S. Lin, J. Chen, X. Weng, L. Yang, X. Chen, *Mater. Res. Bull.* **44**, 1102 (2009)
14. J. Huang, L. Gao, *J. Am. Ceram. Soc.* **89**, 3877 (2006)

15. D. Li, R. Shi, C. Pan, Y. Zhu, H. Zhao, *CrystEngComm* **13**, 4695 (2011)
16. H. Fu, C. Pan, L. Zhang, Y. Zhu, *Mater. Res. Bull.* **42**, 696 (2007)
17. Z. Amouzegar, R. Naghizadeh, H. Rezaie, M. Ghahari, M. Aminzare, *Ceram. Int.* **41**, 8352 (2015)
18. J. Bi, L. Wu, Z. Li, Z. Ding, X. Wang, X. Fu, *J. Alloys Compd.* **480**, 684 (2009)
19. W. Yan, S. ZHANG, L.-w. Zhang, Y.-f. Zhu, *Chem. Res. Chin. Univ.* **23**, 465 (2007)
20. G. Huang, Y. Zhu, *CrystEngComm* **14**, 8076 (2012)
21. Z. Liu, J. Tian, D. Zeng, C. Yu, L. Zhu, W. Huang, K. Yang, D. Li, *Mater. Res. Bull.* **94**, 298 (2017)
22. J. Arin, P. Dumrongrojthanath, O. Yayapao, A. Phuruangrat, S. Thongtem, T. Thongtem, *Superlattices Microstruct.* **67**, 197 (2014)
23. A. Kudo, H. Kato, *Chem. Lett.* **26**, 421 (1997)
24. S. Chatterjee, P. Mahapatra, A. Singh, R. Choudhary, *J. Mater. Sci. Lett.* **22**, 99 (2003)
25. S. Chatterjee, P. Mahapatra, R. Choudhary, A.K. Thakur, *Phys. Stat. Sol. (a)* **201**, 588 (2004)
26. S. Ebraheem, A. El-Saied, *Mater. Sci. Appl.* **4**, 324 (2013)
27. M. Hojamberdiev, G. Zhu, Y. Xu, *Mater. Res. Bull.* **45**, 1934 (2010)
28. R. Dai, Z. Wang, Z. Zhang, Z. Ding, *Surf. Interface Anal.* **46**, 1151 (2014)
29. S. Adhikari, D. Sarkar, G. Madras, *RSC Adv.* **5**, 11895 (2015)
30. G. Huang, Y. Zhu, *Adv. Mater. Sci. Eng. B* **139**, 201 (2007)
31. V. Tsaryuk, V. Zolin, *Spectrochim. Acta A* **57**, 355 (2001)
32. T. Zhang, T. Oyama, A. Aoshima, H. Hidaka, J. Zhao, N. Serpone, *J. Photochem. Photobiol. A* **140**, 163 (2001)